Ab initio study of hydrogen adsorption to single-walled carbon nanotubes

K. Tada,[1] S. Furuya,[1] and K. Watanabe[1,2,3]
[1]*Department of Physics, Science University of Tokyo, 1-3 Kagurazaka, Shinjuku-ku, Tokyo 162-8601, Japan*
[2]*Frontier Research Center for Computational Sciences, Science University of Tokyo, 1-3 Kagurazaka, Shinjuku-ku, Tokyo 162-8601, Japan*
[3]*Core Research for Evolutional Science and Technology (CREST), Japan Science and Technology Corporation, 4-1-8 Honmachi, Kawaguchi, Saitama 332-0012, Japan*
(Received 7 July 2000; published 23 March 2001)

We perform the density-functional and quantum chemical calculations of adsorption of a hydrogen molecule to various kinds of single-walled carbon nanotubes (SWNT's). The potential energy barrier height (PBH) for the dissociative adsorption of a hydrogen molecule onto the outer wall of a nanotube decreases as the tube diameter decreases. In contrast, the PBH for H_2 penetration into an open-ended nanotube increases as the tube diameter decreases, independent of the atomic geometry, i.e., zigzag or armchair structures. H_2, however, cannot adsorb to the inner wall of any type of nanotube. These results on the structure-dependent H_2 adsorption to SWNT's are reasonably explained by the sp^2-sp^3 rehybridization caused by the interaction between the adsorbing hydrogen and carbon atoms of SWNT's.

DOI: 10.1103/PhysRevB.63.155405 PACS number(s): 81.07.−b, 82.20.Kh, 31.10.+z, 31.15.Ar

I. INTRODUCTION

Carbon nanotubes have been intensively studied in anticipation of their application in novel nanoscale materials and device structures, as well as for their fundamental physics.[1] In particular, there has been considerable interest in evaluating the capability of carbon nanotubes as a hydrogen-storage material for clean energy sources. Carbon nanotubes were reported to be very promising candidates for high H_2 uptake.[2,3] Dillon *et al.*[4] measured the H_2 adsorption capacity of single-walled carbon nanotube (SWNT) soot, and the SWNT soot was found to adsorb a large amount of hydrogen.

Monte Carlo simulations based on the model potentials have been performed to determine the optimal carbon nanotube arrays for high H_2 uptake.[5] Darkrim and Levesque[6] studied the influence of the distance between the nearest-neighbor SWNT's on adsorption using the Lennard-Jones potential. Furthermore, Wang and Johnson[7] studied the adsorption of hydrogen gas into SWNT's and the idealized carbon slit pores using model potentials. Comparing the results of this simulation, in which the quantum motion of hydrogen molecules was treated by Feynman's path integral method, with those of classical simulations, gives an indication of the importance of quantum effects in hydrogen adsorption. Quite recently, an elaborate study on hydrogen adsorption and storage in SWNT's and multiwalled nanotubes using the density-functional-based tight-binding calculations[8] has shown that many hydrogen atoms can be stored in the interior and adsorbed to the outer wall of carbon nanotubes, and that the hydrogen storage capacity is limited by the repulsive interactions between H_2 molecules and also those with carbon atoms.

Although these simulations revealed the stable configuration enabling hydrogen storage and the storage capacity, the details of the molecular mechanism of the H_2 reaction with nanotubes in the initial stage of adsorption, in particular, the activation energy barriers for dissociative adsorption of H_2 to carbon nanotube walls, have not been studied. Therefore, the objectives of this paper are to reveal the initial pathways and the interaction potential energies for H_2 adsorption to various nanotubes, and to clarify the underlying electronic states responsible for the adsorption properties, by means of detailed quantum mechanical calculations.

The organization of this paper is as follows. In Sec. II, we describe the method and model for our calculations. In Sec. III, we present the results on the potential energy curves for H_2 adsorption to various nanotubes and discuss the underlying electronic states responsible for the adsorption properties. A summary is given in Sec. IV.

II. METHOD AND MODEL

In the present paper, we perform density-functional calculations based on the supercell method to investigate the adsorption of H_2 onto the outer walls of (3,3), (4,4), and (6,6) SWNT's. We follow the nanotube index (n,m) defined in a previous study.[9] Eight carbon atoms located on the side opposite to the H_2 adsorption sites were fixed and the other atoms were relaxed during the structural optimization. We used the first-principles molecular dynamics method[10,11] with the generalized gradient approximations of PW91 (Ref. 12) and RPBE (Ref. 13) for the exchange-correlation potential. Since the difference between the results obtained with PW91 and those with RPEB was found to be negligible, the results obtained with PW91 will be shown in this paper. The norm-conserving pseudopotentials of NCPS97 (Ref. 14) based on the Troullier-Martins[15] algorithm are used. We expand the electronic wave functions in plane waves up to a kinetic energy of 44 Ry, and choose a Γ point in the Brillouin zone.

The potential energy curves for H_2 penetration into open-ended nanotubes and for H_2 adsorption to the inner walls of nanotubes with various structures and radii have been calculated by the Hartree-Fock method with a PM3 approximation of Gaussian 98.[16] We have also performed a similar calculation for a thin nanotube by the local spin density approximation method and found qualitatively the same result as that with the PM3 approximation. Both edges of the nanotube are

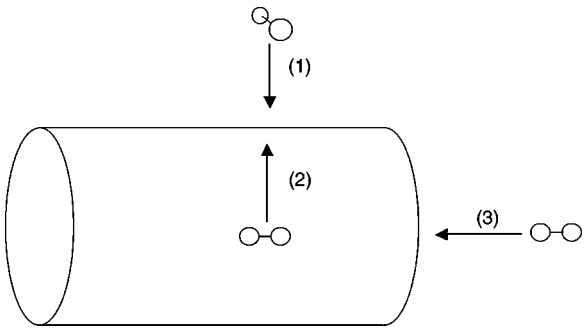

FIG. 1. Configuration of H_2 adsorption to a nanotube considered in the present calculations. (1) Adsorption to outer wall of nanotube, (2) adsorption to inner wall of nanotube, and (3) penetration into nanotube from the open end.

terminated with hydrogen atoms. The configuration of H_2 and the nanotube considered in the present calculation is schematically shown in Fig. 1.

III. RESULTS AND DISCUSSIONS

We describe the interaction potentials of H_2 with various SWNT's for (1) adsorption to the outer wall, (2) adsorption to the inner wall, and (3) penetration into the open ends of nanotubes. First, the potential energies for H_2 on graphene and onto the outer walls of nanotubes of various diameters are given in Fig. 2. The distance is measured from the stable position of the adsorbed site. In the case of graphene, there is no stable site for H_2 adsorption. Thus, the metastable (excited) adsorption site has been chosen as the origin of the horizontal coordinate for graphene.

The potential energy (dash-dotted line) increases as H_2 approaches graphene. This indicates that H_2 cannot adsorb to

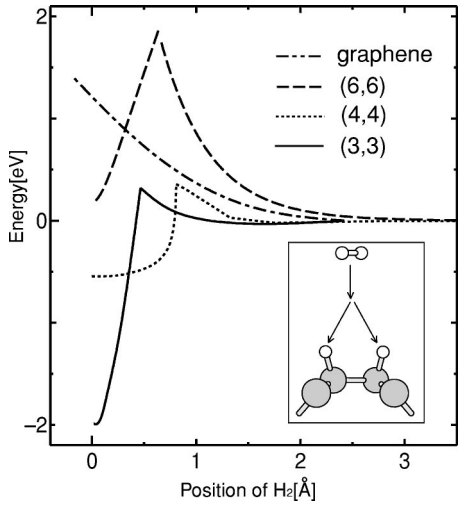

FIG. 2. Potential energy curves for H_2 dissociative adsorption to outer walls of three SWNT's and graphene. A configuration of H_2 and a nanotube used for the calculation is shown in the inset. The abscissa is the distance between the H_2 and the stable position of H_2 adsorbed on the nanotube. The potential energies of H_2 adsorption to graphene (dash-dotted line), (6,6) nanotube (dashed line), (4,4) nanotube (dotted line), and (3,3) nanotube (solid line) are shown.

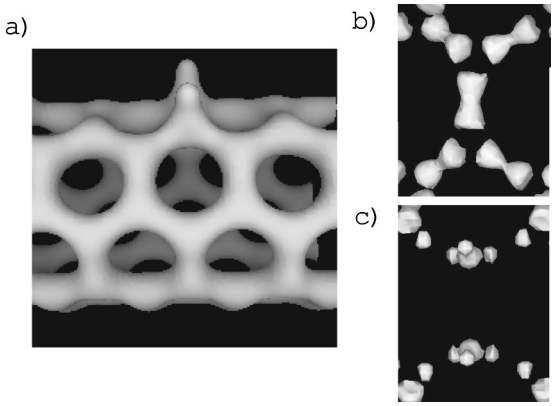

FIG. 3. Valence-electron density of (4,4) nanotube. (a) Side view of the electron density when H_2 is dissociatively adsorbed (protrusions in the upper side) to the nanotube. Top view of the electron density around the adsorption site (b) before and (c) after H_2 adsorption. Rehybridization from (b) sp^2 to (c) incomplete sp^3 bond (C-C bond is weakened) upon H_2 adsorption is seen.

graphene. (Atomic hydrogen can adsorb to graphene without an energy barrier.) However, the potential energies for adsorption to nanotubes (dashed, dotted, and solid lines) increase once and then decrease. The potential energy barrier height (PBH) is found to decrease as the diameter decreases. This means that dissociative adsorption of H_2 to the outer wall of SWNT is likely to occur for thinner nanotubes. It should be noted, however, that H_2 adsorption rarely occurs on thicker nanotubes, in contrast with the adsorption of *atomic* hydrogen, as shown in the previous study.[8]

We have chosen the most probable pathway for dissociative adsorption in the present calculation. That is, the molecular axis of H_2 was assumed to be parallel to the C-C bond in the nanotube. A schematic diagram of the dissociative adsorption of H_2 is given in the inset of Fig. 2. The potential energy and the barrier height may change if another mechanism such as asymmetric dissociation is taken into account. In that case, however, we expect that the characteristic properties of the structure-dependent potential energies would remain unchanged.

To interpret the diameter-dependent adsorption property shown in Fig. 2, we present the valence-electron density of the (4,4) nanotube as an example in Figs. 3(a)–3(c). Figure 3(a) shows the side view of the electron density when H_2 is dissociatively adsorbed (protrusions) on the upper side of the nanotube. Figures 3(b,c) show top views of the electron density for a H_2-free and a H_2-adsorbed nanotube, respectively. The sp^2 nature of graphite is clearly evident in Fig. 3(b). In contrast, it is evident in Fig. 3(c) that sp^3-like bonding among hydrogen and carbon atoms occurred after hydrogen adsorption, although the C-C bond in the center region became weak. This tendency for sp^2-sp^3 rehybridization upon H_2 adsorption is strong for thin nanotubes, because highly *bent* sp^2 bonding of thin nanotubes is favored for the transition to sp^3 bonding. This is the essential reason why the PBH's of (3,3) and (4,4) nanotubes are low compared with that of the (6,6) nanotube. We can understand, for the same

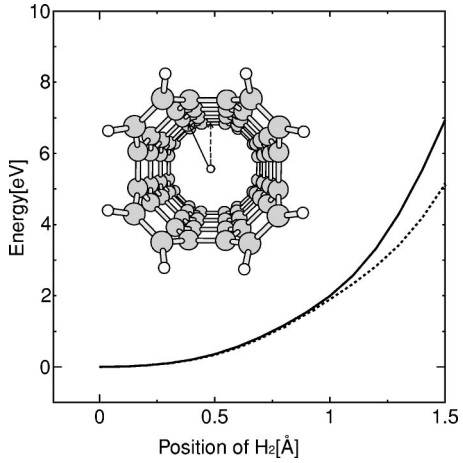

FIG. 4. Potential energy curves for H_2 approaching the inner wall of the (4,4) nanotube [configuration (2) in Fig. 1]. Two paths are chosen (see inset): one is the direction toward a carbon atom (solid line) and the other is that toward the center of the hexagon (dotted line).

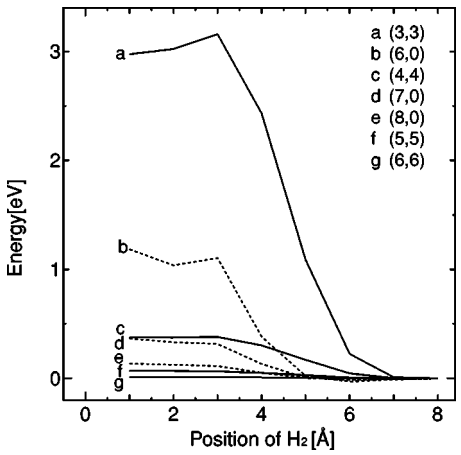

FIG. 5. Potential energies for H_2 penetrating into various types of nanotubes [configuration (3) in Fig. 1]. The solid and dotted curves refer to armchair and zigzag nanotubes, respectively. The abscissa shows the distance between the nanotube center and the H_2 center.

reason, that negligible H_2 adsorbs onto graphene with perfect sp^2 bonding without bending.

Next, we show the potential energies for H_2 adsorption to the inner wall of the (4,4) nanotube in Fig. 4. The potential energies of H_2 as a function of the distance of the H_2 from the nanotube axis perpendicular to the inner wall, as shown in the inset, are given. The potential energies along the two lines, one toward a carbon atom (solid line) and the other toward the center of the hexagon (dotted line), increase. This feature is also understood from the tendency in the electronic transition from sp^2 to sp^3 bonding discussed above. In contrast with adsorption to the outer wall, sp^3 bonds cannot be formed upon adsorption to the inner walls because the carbon atoms bend oppositely (see the inset of Fig. 4) which prevents them from forming sp^3 bonds. Therefore, H_2 remains only on the nanotube axis once it enters into the nanotube. This feature is compatible with the previous result[8] on hydrogen storage inside SWNT's.

Finally, the potential energies for H_2 entering into various nanotubes are given in Fig. 5. The abscissa is the distance between the nanotube center and H_2. A common feature of these curves is that the potential energy increases and flattens after passing under the nanotube edge. The PBH decreases as the diameter of the nanotube increases. As is clearly evident, the PBH abruptly decreases when the diameter goes beyond 5.7 Å [(4,4) nanotube]. This is because the wave functions of carbon atoms and that of H_2 do not overlap significantly for thicker nanotubes. To see the structure-dependent PBH for H_2 penetration into the open-ended nanotubes, we plot, from Fig. 5, the PBH as a function of the diameter of the nanotube in Fig. 6. It is very interesting to note that the data for seven nanotubes (circles and rectangles refer to armchair and zigzag nanotubes, respectively) fall almost on a single curve. This result indicates that the PBH depends only on the diameter and not on details of the geometrical structure, such as whether the nanotube is an armchair or zigzag type. The reason is simple: H_2 interacts equally with carbon and hydrogen atoms on the edge and, thus, is subjected to the potential formed by the averaged electronic structures of the nanotubes. We reasonably expect, from Fig. 6, that the PBH for H_2 penetration into typical SWNT's with diameters larger than 1 nm is negligible and, thus, H_2 can easily enter into the empty space inside SWNT's. This is in agreement with the experimental observation by Raman spectroscopy.[8]

The present results of quantum-mechanical simulations enable us to stress that the properties of nanotube-structure dependent H_2 adsorption are completely different for different adsorption pathways, i.e., on the outer wall, inner wall, and penetration into the open end of SWNT's, due to the local electronic states near the adsorption sites. The characteristics in the initial stage of adsorption clarified in this paper must influence the H_2 storage property such as the optimized nanotube arrays for high-H_2 uptake.[6,7] Further study is

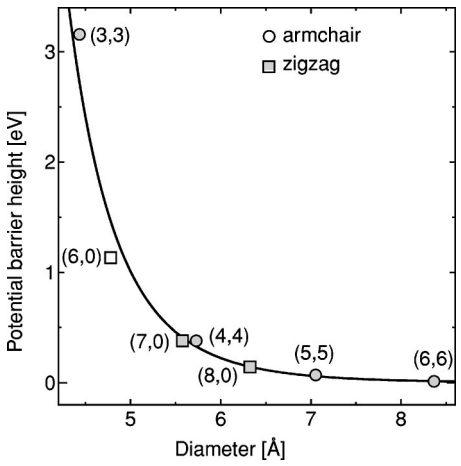

FIG. 6. Potential energy barrier height for H_2 penetrating into the nanotube as a function of the diameter of the nanotube. Open circles and open squares indicate armchair and zigzag nanotubes, respectively. The solid line is obtained from the least-squares fit of the seven data values.

necessary to reveal the correlation between the H_2 molecular reaction in the initial stage of adsorption and the statistical property of H_2 storage in carbon nanotubes.

IV. CONCLUSION

We have studied the adsorption of H_2 to SWNT's with various diameters and structures, using the density functional and quantum chemical calculations to elucidate the initial reaction pathways and the underlying electronic states. The PBH for dissociative adsorption of H_2 onto the outer wall of the nanotube decreases as the diameter decreases. H_2, however, cannot adsorb to the inner wall of the nanotube. We also found that the PBH for H_2 penetration into the open-ended nanotube decreases as the tube diameter increases, which is independent of the atomic structure of nanotubes. The structure-dependent properties obtained are explained in terms of the different degrees of sp^3 bond formation upon H_2 adsorption and of wave-function overlap between H_2 and the nanotube for H_2 penetration.

We believe our results contribute to an understanding of the molecular processes and the microscopic origin in the initial stage of hydrogen storage in SWNT's.

ACKNOWLEDGMENTS

K.T. thanks the Science University of Tokyo for the use of FACOM VPP5000 and the Supercomputer Center, Institute for Solid State Physics, University of Tokyo, for the use of the facility.

[1] See, e.g., *Science and Application of Nanotubes*, edited by D. Tománek and R. J. Enbody (Kluwer Academic/Plenum Publishers, New York, 2000).
[2] P. Chen, X. Wu, J. Lin, and K. I. Tan, Science **285**, 91 (1999).
[3] C. Liu, Y. Y. Fan, M. Liu, H. Liu, H. T. Cong, H. M. Cheng, and M. S. Dresselhaus, Science **286**, 1127 (1999).
[4] A. C. Dillon, K. M. Jones, T. A. Bekkedahl, C. H. Kiang, D. S. Bethune, and M. J. Heben, Nature (London) **386**, 377 (1997).
[5] K. G. Ayappa, Chem. Phys. Lett. **252**, 59 (1998).
[6] F. Darkrim and D. Levesque, J. Chem. Phys. **109**, 4981 (1998).
[7] Q. Wang and J. K. Johnson, J. Chem. Phys. **110**, 577 (1999).
[8] S. M. Lee, K. S. Park, Y. C. Choi, Y. S. Park, J. M. Bok, D. J. Bae, K. S. Nahm, Y. G. Choi, S. C. Yu, N. Kim, T. Frauenheim, and Y. H. Lee, Synth. Met. **113**, 209 (2000).
[9] R. Saito, M. Fujita, G. Dresselhaus, and M. S. Dresselhaus, Appl. Phys. Lett. **60**, 2204 (1992).
[10] M. C. Payne, M. P. Teter, D. C. Allan, T. A. Arias, and J. D. Joannopoulos, Rev. Mod. Phys. **64**, 1045 (1992).
[11] G. Kresse and J. Furthmüller, Phys. Rev. B **54**, 11 169 (1996).
[12] J. P. Perdew, J. A. Chevary, S. H. Vosko, K. A. Jackson, M. R. Pederson, D. J. Singh, and C. Fiolhais, Phys. Rev. B **46**, 6671 (1992).
[13] B. Hammer, L. B. Hansen, and J. K. Nørskov, Phys. Rev. B **59**, 7413 (1999).
[14] K. Kobayashi, Comput. Mater. Sci. **14**, 72 (1997).
[15] N. Troullier and J. L. Martins, Phys. Rev. B **43**, 1993 (1991).
[16] GAUSSIAN 98, Revision A.7, M. J. Frisch, G. W. Trucks, H. B. Schlegel, G. E. Scuseria, M. A. Robb, J. R. Cheeseman, V. G. Zakrzewski, J. A. Montgomery, Jr., R. E. Stratmann, J. C. Burant, S. Dapprich, J. M. Millam, A. D. Daniels, K. N. Kudin, M. C. Strain, O. Farkas, J. Tomasi, V. Barone, M. Cossi, R. Cammi, B. Mennucci, C. Pomelli, C. Adamo, S. Clifford, J. Ochterski, G. A. Petersson, P. Y. Ayala, Q. Cui, K. Morokuma, D. K. Malick, A. D. Rabuck, K. Raghavachari, J. B. Foresman, J. Cioslowski, J. V. Ortiz, A. G. Baboul, B. B. Stefanov, G. Liu, A. Liashenko, P. Piskorz, I. Komaromi, R. Gomperts, R. L. Martin, D. J. Fox, T. Keith, M. A. Al-Laham, C. Y. Peng, A. Nanayakkara, C. Gonzalez, M. Challacombe, P. M. W. Gill, B. Johnson, W. Chen, M. W. Wong, J. L. Andres, C. Gonzalez, M. Head-Gordon, E. S. Replogle, and J. A. Pople (Gaussian, Inc., Pittsburgh PA, 1998).